

Small-angle neutron scattering · Contrast variation · Carbon black · Graphitic shell · Quasirodlike aggregates

We have been exploring the use of small-angle neutron scattering and the method of contrast variation to give a new look at very old problem – reinforcement of elastomers by carbon black in durable rubber products. It was found that in an experimental carbon black, HSA, the aggregates are quasirodlike, containing an average of 4–6 particles. The aggregates have an outer graphitic shell and an inner core of lower density carbon. The core is continuous throughout the carbon black aggregate. Contrast variation of swollen HSA-polyisoprene gels shows that the HSA is completely embedded in polyisoprene. The agglomerates are formed predominantly by end-on associations of the rodlike aggregates. The surface structure of the carbon black appears smooth over length scales above about 1 nm. Further studies on production carbon blacks suggest that the shell-like aggregate structure is present in commercial carbon blacks.

Die Struktur von Ruß und seine Verbindungen in Elastomermischungen: Eine Studie anhand von Neutronenstreuung

Kleinwinkelneutronenstreuung · Kontraständerung · Graphithülle · Propfenförmige Aggregate

Wir haben die Verwendung von Kleinwinkelneutronenstreuung und die Methode der Kontraständerung untersucht, um einen neuen Blick auf ein sehr altes Problem zu werden – Verstärkung von Elastomeren durch Ruß in langlebigen Kautschukprodukten.

Die Untersuchungen ergaben propfenförmige Aggregate aus durchschnittlich 4–6 Teilchen. Die Aggregate besitzen außen eine Graphithülle und einen inneren Kern aus weniger dichtem Kohlenstoff. Der Kern zieht sich kontinuierlich durch das Rußaggregat. Kontraständerungen von gequollenem HSA-Polyisopren zeigen, daß HSA vollständig in das Polyisopren eingebettet ist. Die Agglomerate werden bevorzugt durch end-on-Verknüpfungen der propfenförmigen Aggregate gebildet. Die Oberflächenstruktur des Rußes erscheint über Bereiche von über 1 nm glatt. Weitere Untersuchungen bei der Rußherstellung legen nahe, daß die hüllenartige Aggregatstruktur auch in kommerziellen Rußen vorhanden ist.

The Structure of Carbon Black and its Associations in Elastomer Composites: A Study using Neutron Scattering

R. P. Hjelm, Los Alamos (USA), W. Wampler and M. Gerspacher, Fort Worth (USA)

Carbon black (CB)-elastomer composites are examples of "classical systems" of heterogeneous microphases of matrix and reinforcement. The carbon black consists of a hierarchy of structures in which spheroid particles are fused into aggregates which associate by van der Waal's forces to form agglomerates. There is a substantial body of work on CB structures and CB-elastomer composites. Even so, nearly 100 years after the discovery of the effect of CB on rubber, there is controversy on what the reinforcing mechanism is. Ideas center on particle size and surface structure relating to associations with the elastomer, aggregate shape and the extent and morphology of agglomerates. In the interactions with the elastomer, the strength of the CB-polymerbinding and polymer chain configuration and entanglements are considered highly important. A clearer understanding of the mechanical properties of reinforced rubber requires a better picture of the structure of the material and its components *in situ*.

Our objective is to provide structural information on CB and CB-elastomer composites. This includes the morphology and internal structure of CB particles and aggregates; the association of aggregates in rubber composites; and the associations of elastomer and carbon blacks. We also need to show the generality of the structural features in different carbon blacks having different mechanical properties when composited with rubber. In this paper we discuss the structure of aggregates as probed by neutrons.

Small-angle neutron scattering

Small-angle neutron scattering (SANS) is an important technique for structural

characterization. The basic physical concept behind neutron scattering is the same as for electrons or x-rays. However, for neutrons, the scattering is produced almost entirely by interactions with the nuclei. These interactions are very small relative to that of an electron or an x-ray, consequently the neutrons are relatively more penetrable, allowing studies of materials in the bulk or in containment for special environments. An important aspect of the scattering of neutrons is that the neutron scattering lengths, the measure of scattering amplitude, are not monotonic with atomic number (Table I), unlike electrons or x-rays. Consequently, there is substantial contrast for neutron scattering among light elements. Further, there are often significant differences among the scattering lengths of isotopes of the same element. The difference between hydrogen and deuterium (Table I) is particularly important in this regard.

The SANS signal derives from fluctuations in the scattering length density, $\rho(r)$, as a function of position, r , in the sample. The $\rho(r)$ is calculated by summing the scattering lengths of the atoms (see Table I) in a volume at r , then dividing by the value of that volume. Thus, $\rho(r)$ both density and chemical composition. The intensity of scattering from $\rho(r)$ is given by a Fourier transform-squared relationship,

Table I. Scattering Lengths of Some Light Elements and Hydrogen Isotopes

Element	Scattering length (fm)
¹ H	-3.7403
² D	6.675
C	6.6484
N	9.2600
O	5.8050

$$I(Q) = K \left\langle \left| \int \rho(r) \exp(-i r \cdot Q) d r \right|^2 \right\rangle \quad (1)$$

The expression in the angle brackets is the spherical averaged particle form factor, $\langle P(Q) \rangle$. If we consider the scattering from particles in a fluid, the constant, K , is proportional to $\Delta \rho^2$, $\Delta \rho = \bar{\rho}_p - \rho_s$, which is the contrast between the average scattering length density of the particle, $\bar{\rho}_p$, and the that of the fluid, ρ_s .

In our experiments, the scattered intensity, $I(Q)$, was measured as the absolute differential cross section per unit scattering mass ($\text{cm}^2 \text{mg}^{-1}$) as a function of the magnitude of the scattering vector, Q . For elastic scattering events, $Q = (4 \pi / \lambda) \sin \theta$, where λ is the neutron wavelength and θ is half the scattering angle. The wavelength of neutrons used in LQD, the SANS instrument used in these studies, is of order 1 to 10 Å. Thus, the values of Q over which these measurements were made probe length scales on the order of a 10 to several hundreds of Å (length scales $\sim Q^{-1}$).

Particle structure characterization

Again, considering the case of particles in a medium, the size and scattering mass of the scattering body can be determined by Guinier approximation,

$$I(Q) = \frac{\phi V_p^2 \Delta \rho^2}{M} \exp\left(-\frac{Q^2 R_g^2}{3}\right) \quad (2)$$

which applies over the domain $Q < R^{-1}$, where R is the average radius of the particles. In Eq. (2), ϕ is the volume fraction of particles, each with volume V_p , mass, M , and radius of gyration, R_g . The models may be refined by fitting the observed scattering, over a wide range of Q , to a particle form factor (Eq. (1)).

Over length scales such that $QR \gg 1$ the scattering can be described as a power-law:

$$I(Q) = I_0 Q^{-\alpha} \quad (3)$$

Here, α and I_0 are constants, with the value of α being indicative of the surface "smoothness". For the special case of smooth interfaces, $\alpha = 4$ and the scattering is termed Porod-Scattering. In this

case, $I_0 = 2 \pi S \Delta \rho^2$, where S is the interfacial area per unit volume of the sample.

In the case where there are particle interactions, so that the positions and/or orientations are correlated in some way, it is necessary to reinterpret Eq. (1) as

$$I(Q) = S'(Q) \langle P(Q) \rangle \quad (4)$$

In this expression $S'(Q)$ is the effective structure factor resulting from particle correlations in solution. The effective structure factor can be formulated to take into account non-spherical, polydisperse particles.

Contrast variation

SANS provides unique capabilities for the study of composite materials. However, scattering intensity measured by SANS does not have unambiguous spatial information due to the loss of phase information in the measured $I(Q)$ (Eq. (1)). We have outlined a means of recovering spatial information in composite materials by the method of contrast variation [2, 3]. In this method, we change $\Delta \rho^2$ (Eqs. (1)

and (2)) by suspending the sample in different mixtures of deuterated and protonated fluid (Fig. 1). Originally developed for research in the structure of biological particles in solution [4], the method can be used to contrast out one or another of the components in a complex mixture. Alternatively, it can be used to distinguish the internal structure from the shape of one component – say, CB. We implemented this approach in studies of CB and CB-elastomer composites. The CB-elastomer composites were prepared as "bound" rubber [3], which remains after extensive high temperature extraction with good solvents. This material is dried and swelled with cyclohexane with different weight fraction of deuterocyclohexane, $f_{C_6D_{12}}$.

For a homogeneous solution of noninteracting particles, the scattering has a welldefined behavior given by,

$$I(Q) = \Delta \rho^2 I_\Omega(Q) + \Delta \rho I_{\Omega\xi}(Q) + I_\xi(Q) \quad (5)$$

The basic scattering function, $I_\Omega(Q)$ arises from the solvent-excluding parts of the structure, $\Omega(r)$. The second one,

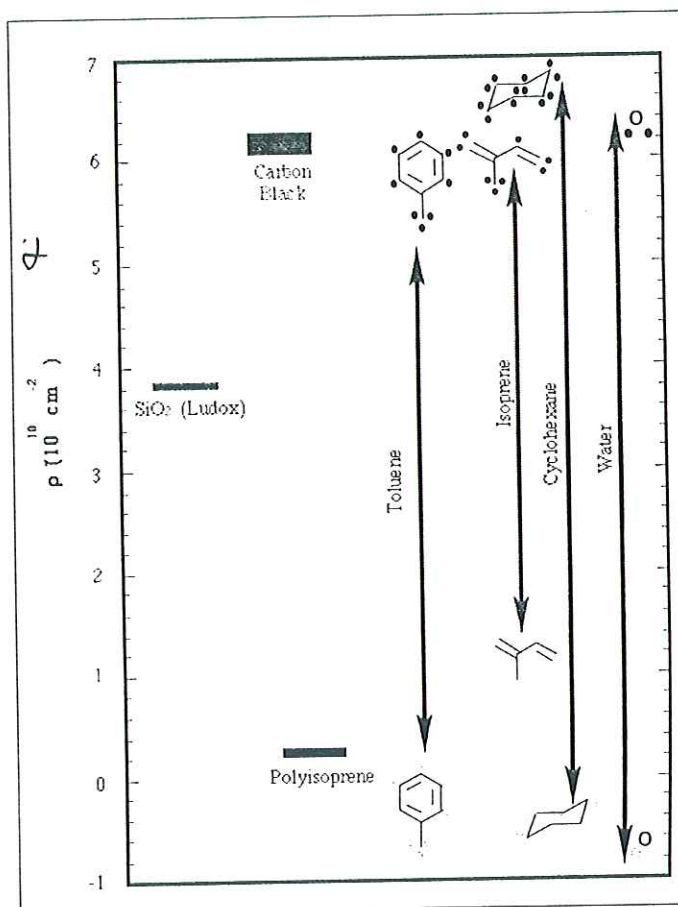


Fig. 1. Scattering length density of carbon black, silica and polyisoprene compared to various mixtures of deuterated and protonated solvents.

$I_{\zeta}(Q)$, represents scattering from the internal fluctuations, $\zeta(r)$. The last function, $I_{\Omega\zeta}(Q)$, is the scattering due to correlations between $\Omega(r)$ and $\zeta(r)$. In this representation, the structure is defined as the sum of the shape and internal structure terms; thus,

$$\rho(r) = \rho_s + \Delta \rho \Omega(r) + \zeta(r) \quad \text{Eq. (5)}$$

is an approximation for heterogeneous systems, such as studied here, as the different terms are complex statistics of the different contrasts present in the sample [4]. We define $\Delta \rho = 0$ as the contrast match point.

The Guinier approximation (Eqs.(2)) can be applied in the method of contrast variation. The contrast dependence of the intensity at $Q = 0$ is,

$$(I(0))^{1/2} = \sqrt{\frac{\phi}{M}} V_p \Delta \rho \quad (6)$$

and

$$R_g^2 = R_c^2 + \frac{\alpha}{\Delta \rho} - \frac{\beta}{\Delta \rho^2} \quad (7)$$

for the contrast dependence of R_g . In Eq.(7) R_c is the radius of gyration of $\Omega(r)$, α is proportional to the second moment of $\zeta(r)$ and β is proportional to the square of the first moment of $\zeta(r)$. Thus, the contrast variation method provides five structural parameters based on the Guinier analysis: Volume and $\bar{\rho}_p$, from the changes that occur in $I(0)$ with ρ_s , and the three parameters in Eq.(7). Again, in chemically heterogeneous systems statistical averages replace the form in Eqs. (6) and (7) are replaced a statistical averages [4].

Carbon black structure in suspension and with elastomer

For our studies, we used the experimental carbon black, HSA. There are substantial changes in the neutron scattering of HSA and HSA-polyisoprene (HSA-PI) gels with, $f_{C_6D_{12}}$ (Fig. 2).

The results of the contrast-dependent Guinier analysis (Eqs.(6) and (7) for the HSA sample are summarized in Table II. The large value of α is highly significant: it shows that the particles have a shell-core structure, with an outer shell of density like that of graphite, consistent with TEM [1] and scanning tunneling microscopy [7]. The core of the particle has density like that of amorphous carbon,

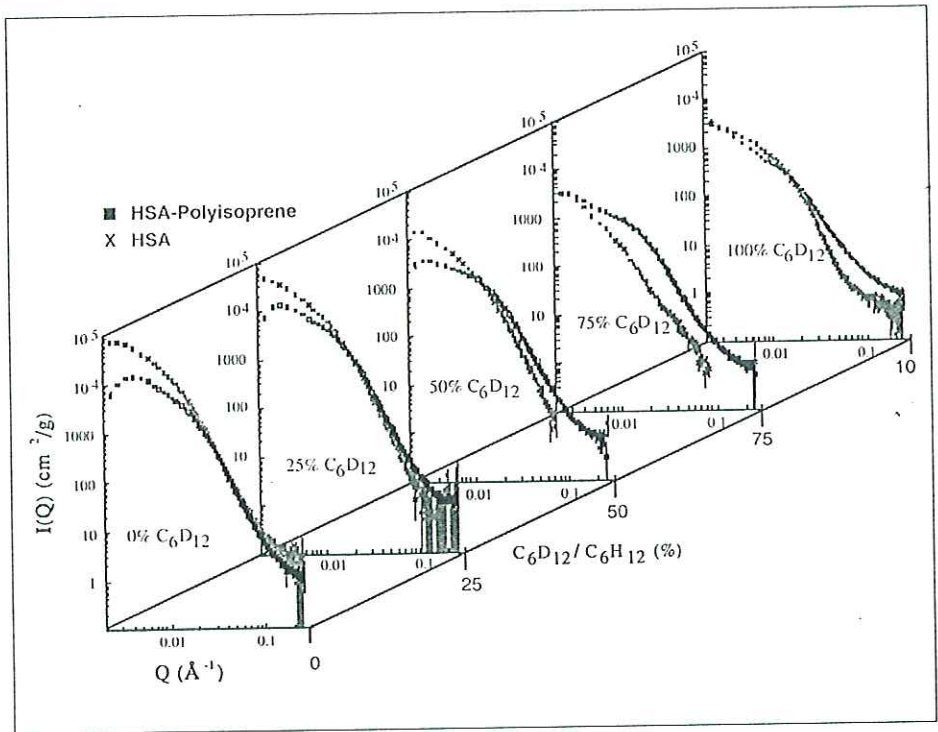


Fig. 2. SANS of HSA-polyisoprene Composite Gels and HSA Suspended in different Fractions of Deuterocyclohexane Data: \times , HSA; \blacksquare , HSA-polyisoprene composite gel.

Table II. Structural Parameters for HSA

V_p (nm ³)	$\bar{\rho}_p$ (cm ⁻²)	R_c (nm)	α	S (m ² g ⁻¹)
5.4 (3) 10 ⁴	5.7 (0.3) 10 ¹⁰	29.3 (4)	2.0 (3) $\times 10^{-2}$	170 (4)

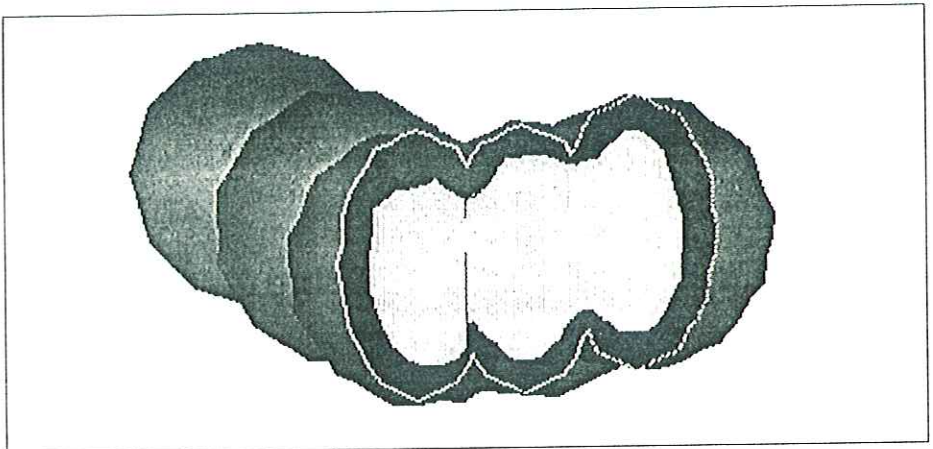


Fig. 3. Schematic of the Carbon Black Aggregate Structure: The structure consists of a linear array of spheroid particles. The average aggregation number is 4 to 6 with particle sizes being in the range of 240 to 290 Å. The outer shell of the structure (black) consists of graphitic carbon crystallites, with a core (gray) of less dense void-filled (white) carbon.

but with voids. Most significantly, the particles are fused together so that the amorphous cores, are continuous in the aggregate. $I_{\Omega}(Q)$ determined using Eq. (5) was fitted to a prolate ellipsoid of revolution showing that the aggregates are approximately 29 nm by 150 nm and are rodlike,

having little branching, with 5 to 6 particles on average. This result is consistent with stereo TEM studies. [6] Finally, $I_{\Omega}(Q)$ obeys Porod's Law (Eq. (3)); thus the particles have smooth surfaces, the surface area of which is shown in Table II, on length scales greater than 1 to 2 nm.

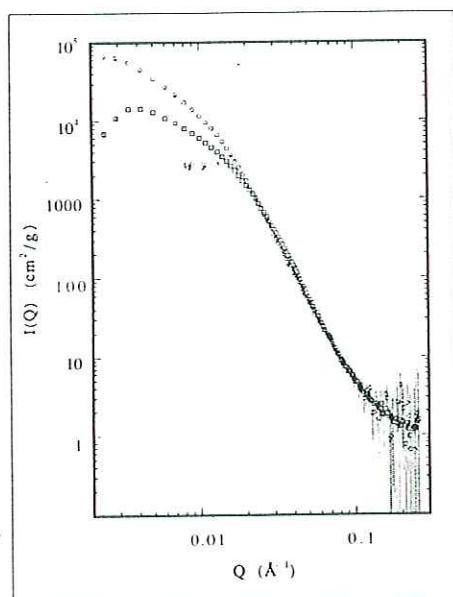


Fig. 4. Comparison of Scattering from HSA suspensions and Gels of Bound Rubber Computed for $f_{C_6D_{12}} = 0.07$: Data: \circ , HSA; \square , HSA-polyisoprene.

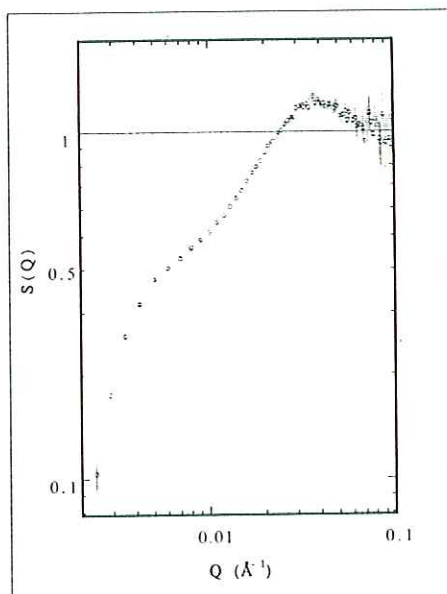


Fig. 5. Structure factor from the scattering of HSA in the Composite Gel of Bound Rubber: Calculated values: \circ .

These conclusions are summarized in schematic form in Fig. 3. Studies on the production CB's, N299, N330 and XLH81 suggest that the shellcore structure found in HSA is present in these CB's, as well.

These conclusions have important implications on the mechanism of reinforcement of HSA. Ideas about rubber composite properties must take into account the short, rigid rodlike character of the carbon black aggregates. Further, the mechanism of polymer binding must take into account the upper limit of the length scale for CB surface roughness [8] determined from the SANS studies.

The SANS of HSA-polyisoprene bound rubber gels is significantly different from that of HSA alone (Fig. 2). These data, too, can be fit using Eq. (5). When Q is less than approximately 10 \AA^{-1} , the fits suggests a minimum at a $\Delta \rho$ near the $\bar{\rho}_p$ value for HSA (Table II) [2]. For Q greater than 10 \AA^{-1} there is a shift in the $\Delta \rho$ for the minimum scattering intensity towards the computed $\bar{\rho}$ of $3.2 \cdot 10^{10} \text{ cm}^{-2}$ of the composite, implying that the contrast for CB is from the solvent-polyisoprene mixture on these length scales ($\sim Q^{-1}$). Thus, CB is almost completely coated with elastomer.

The scattering at $f_{C_6D_{12}} = 0.07$, where only CB scattering should be observed, can be calculated from the data in

Fig. 2 by interpolation using Eq. (5). The result of this calculation is shown in Fig. 4. For $Q < 0.02 \text{ \AA}^{-1}$ the scattering from HSA is considerably greater than that from the HSA-polyisoprene composite. For Q between 0.02 \AA^{-1} and 0.07 \AA^{-1} the HSA intensity is slightly less than that of the composite. The scattering from the two samples becomes indistinguishable for Q greater than 0.07 \AA^{-1} . We have shown [2] that the scattering from HSA alone in suspension (Fig. 2) is very close to that expected from non-interacting particles. Thus, we use Eq. (4) to calculate $S'(Q)$, the result of which is shown in Fig. 5. Some features of $S'(Q)$ probably arise from the fact that the CB aggregates are elongated. That $S'(Q)$ is significantly smaller than unity at low Q implies that there is strong exclusion of CB particle neighbors in the HSA-PI composite. It is likely then that on average each CB aggregate is separated by a considerable amount of polymer that prevents the aggregate from making lateral associations. On the other hand the amount of CB in this sample, 65% by weight in the dried, extracted material, is above the percolation limit. Thus, the CB aggregates must be touching or nearly so, in which case these results suggest end on association of the rodlike aggregates.

When the incoherent backgrounds are accounted for, the scattering in the calculated at $f_{C_6D_{12}} = 0.07$ (Fig. 4) falls off as Porod's law (Eq. (3)) for $Q < 0.02 \text{ \AA}^{-1}$. This observation indicates that smooth surfaces are also present in HSA in the solvent-impregnated polyisoprene. The scattering in this same Q -domain from samples near to the HSA contrast match point fall off with power laws in Q (Eq. (3)) intermediate between -4 and -3 . This observation suggests that the surface of the contrasted particles appear rough at high polyisoprene contrasts. This can be interpreted as being from interpenetrating solvent and polyisoprene-rich phases that surround the HSA-PI aggregates.

Acknowledgments

This work was supported by the Office of Basic Energy Sciences of the Department of Energy. This work benefited from the use of the Low- Q Diffractometer at the Manuel Lujan Neutron Scattering Center of the Los Alamos National Laboratory which is supported by the Office of Basic Energy Sciences of the United States Department of Energy under contract W-7405-ENG-36 to the University of California.

References

- [1] W.H. Hess and C.R. Herd, Carbon Black, Donnet, ed Dekker, New York, 1993 91.
- [2] R.P. Hjelm, W. Wampler, P.A. Seeger and M. Gerspacher, J. Mat. Res., **9** (1994) 3210.
- [3] R.P. Hjelm, W. Wampler and M. Gerspacher, Mat. Res. Soc. Symp. Proc., **376** (1996) 303.
- [4] R.P. Hjelm, J.T. Mang, C. Skidmore und M. Gerspacher, Proceedings of the Workshop on Materials Research Using Cold Neutrons at Pulsed Sources, World Scientific Publishing (1999) 120.
- [5] K. Ibel and H.B. Stuhmann, J. Mol. Biol., **93** (1975) 255.
- [6] T.C. Gruber, T.W. Zerda and M. Gerspacher, Carbon, **31** (1993) 1209.
- [7] J.-B. Donnet and E. Custodero, at Carbon, **30** (1992) 813.
- [8] T.W. Zerda, H. Yang and M. Gerspacher, Rubber Chem. Technol., **65** (1992) 130.

Corresponding author:
Rex P. Hjelm
MLNSC
Los Alamos National Laboratory
Los Alamos
NM 87545
USA